scientific reports

Check for updates

OPEN

Algorithm of quantum engineering of large-amplitude high-fidelity Schrödinger cat states

Mikhail S. Podoshvedov[1,2], Sergey A. Podoshvedov[1]✉ & Sergei P. Kulik[1,3]

We present an algorithm of quantum engineering of large-amplitude $\geq$ 5 high-fidelity $\geq$ 0.99 even/odd Schrödinger cat states (SCSs) using a single mode squeezed vacuum (SMSV) state as resource. Set of *k* beam splitters (BSs) with arbitrary transmittance and reflectance coefficients sequentially following each other acts as a hub that redirects a multiphoton state into the measuring modes simultaneously measured by photon number resolving (PNR) detectors. We show that the multiphoton state splitting guarantees significant increase of the success probability of the SCSs generator compared to its implementation in a single PNR detector version and imposes less requirements on ideal PNR detectors. We prove that the fidelity of the output SCSs and its success probability are in conflict with each other (which can be quantified) in a scheme with ineffective PNR detectors, especially when subtracting large (say, 100) number of photons, i.e., increasing the fidelity to perfect values leads to a sharp decrease in the success probability. In general, the strategy of subtracting up to 20 photons from initial SMSV in setup with two BSs is acceptable for achieving sufficiently high values of the fidelity and success probability at the output of the generator of the SCSs of amplitude $\leq$ 3 with two inefficient PNR detectors.

In quantum optics the notion of the superposition of classically distinguishable macroscopic states[1] finds its embodiment in a form of superposition of coherent states with amplitudes equal in magnitude but opposite in sign[2,3]. Macroscopic SCSs can be of great significance in the demonstration of the fundamental problems[4,5]. In addition, the superpositions are well adjusted for the implementation of the quantum protocols[6–13]. The interaction of two coherent states with amplitudes equal in magnitude on a balanced beam splitter guarantees an increase in the modulus of one coherent state by $\sqrt{2}$ times, while, at the same time, leaving the other output mode in the vacuum state $\left(|\beta\rangle|\beta\rangle \rightarrow |\sqrt{2}\beta\rangle|0\rangle\right)$. Furthermore, mixing of the components of entangled coherent states on the balanced BS separates them on their parity assuming that the vacuum state is an even state[6,7,9]. This allows for nearly deterministic implementation of Bell state measurement by means of two PNR detectors. To reduce contribution of an event when both PNR detectors are silent which may occur, SCSs of amplitude $\beta \geq 2$ are required to provide the sufficiently high degree of orthogonality[9] of the coherent states $|\pm\beta\rangle$. As quantum protocols work on the principle of producing the required state with subsequent measurement to obtain information stored in the prepared state, it is not surprising that the need to put into practice bright nonclassical continuous variable (CV) states especially including high-amplitude SCSs as well as entangled both with each other and with the photonic states (hybrid states) provoked a fairly large drive[14–32]. So, entangled coherent states can be realized by passing pure SCSs through the balanced BS. Development of advanced technologies of quantum engineering of nonclassical states can be used to implement more complex entangled states with more than two distributed coherent nodes.

Practical realization of the optical SCSs mainly relies on nondeterministic photon subtraction technique, being the key for quantum engineering of the nonclassical CV states. The first implementation of the technique is based on passage of a Gaussian quantum state through highly transmitting beam splitters[14] (HTBS). By detecting photons in the measurement channel, catlike state may be generated in the output channel. But the detection of photons diverted by such HTBS into the measuring mode becomes a fairly rare event even in the case of small values of the SCS amplitude $\beta \leq 2$. Undoubtedly, given the serious progress in PNR detection based on transition-edge sensor (TES) technology[33–37], further modification of the photon subtraction technique could go in the direction of increase of number of subtracted photons[17,18,21,22,29–32], as well as using BS with arbitrary

[1]Laboratory of Quantum Engineering of Light, South Ural State University (SUSU), Chelyabinsk, Russia. [2]Institute of Physics, Kazan Federal University (KFU), Kazan, Russia. [3]Quantum Technology Centre, M.V. Lomonosov Moscow State University, Moscow, Russia. ✉email: sapodo68@gmail.com

parameters[29–32] to have a chance to enhance output state characteristics. So, TES detector in[36] has a near unity detection efficiency and feature resolution below 20 photons at $1535nm$ but can detect up to 100 photons with a few-photon uncertainty which makes it appropriate to take theoretical consideration of subtracting one hundred and even more photons from the initial Gaussian SMSV state. In general, despite a number demonstrations of the SCS prototypes[16,18,19,21,26–28], the problem of generating large-amplitude with $\beta \geq 2$ even/odd SCS states remains challenge the solution of which can give impulse for the practical implementation of quantum protocols with coherent states. Here, we use a hub of k sequentially arranged BSs with arbitrary transmission and reflection amplitudes in each measuring mode which PNR detector is set to generate measurement-induced even/odd SCSs. As a component from which the target state is generated, the SMSV is applied as a state that is routinely used in practice. Moreover, use of the SMSV as input to the hub is quite natural as the state has even parity as well as the even SCS and can approximate it with sufficiently high fidelity for small amplitudes $\beta \leq 1$[23]. First, we introduce a family of CV states of a certain parity realized by the hub by means of subtraction of arbitrary number of photons from the SMSV state. The parity of the number of photons extracted from the SMSV in an indistinguishable manner determines the parity of the generated states. We show the family of the CV states of certain parity depends on one parameter. Second, we numerically demonstrate a possibility of generating even/odd SCSs amplitudes $\beta \geq 5$ with a fidelity exceeding > 0.99 (so-called perfect values) at the exit from the hub in the case of subtraction of 90, 91 photons from the initial SMSV by ideal PNR detectors. Third, we show advantage of using multiphoton state demultiplexing[37] resulting in a significant gain in the success probability of generating the SCSs on compared to the case of redirecting the multiphoton state into one PNR detector. In addition, the use of several PNR detectors reduces the requirements on maximum number of measurable photons detected with single-photon resolution. Fourth, we show that the characteristics (fidelity and success probability) of the output SCSs compete with each other in the practical case of using imperfect PNR detectors, which to a large extent can prevent the creation of a larger amplitude SCSs generator when it is required to subtract large number (say, 100) of photons. To avoid the competition, it is required to extract a smaller (say, 20) number of photons to guarantee obtaining close-to-ideal values of the output parameters.

Results

Perfect values of even/odd SCSs parameters at the hub exit. Let us consider the passage of SMSV state through a system of $k > 0$ lossless beam splitters BSs (BS_i) with real transmittance $t_i > 0$ and reflectance $r_i > 0$ coefficients ($i = 1, \ldots, k$) satisfying the normalization condition $t_i^2 + r_i^2 = 1$ and arranged in a row one after another, as shown in Fig. 1. No other states (vacuum) are applied to the second input of each beam splitter. In Fig. 1, the SMSV state occupies zero mode while the auxiliary modes denoted by $i (i = 1, 2, \ldots, k)$ are terminated by k PNR detectors. The original SMSV state is given by.

$$|SMSV\rangle = \frac{1}{\sqrt{\cosh s}} \sum_{n=0}^{\infty} \frac{y_0^n}{\sqrt{(2n)!}} \frac{(2n)!}{n!} |2n\rangle, \tag{1}$$

where the parameter $s > 0$ is the squeezing amplitude of the SMSV state defining amount $y_0 = \tanh s/2 \leq 0.5 \geq 0$. It follows from formula (1) the SMSV state is described by two parameters s and y_0, respectively. Furthermore, the input state in Eq. (1) can also be characterized by two more parameters, namely, the squeezing S expressed in dB as $S = -10log\left(exp(-2s)\right)$ and the mean number of photons $\langle n\rangle_{SMSV} = sinh^2 s$ in the state. The absence of input SMSV (vacuum) is determined by the values $s = 0$, $y_0 = 0$, while the value of $y_0 = 0.5$ corresponds to the non-physical case of an infinitely large squeezing amplitude $s \to \infty$ of the original SMSV. The optical scheme in Fig. 1 can be considered as a hub composing of k elements. Each $i-$ element of the hub consists of one BS and

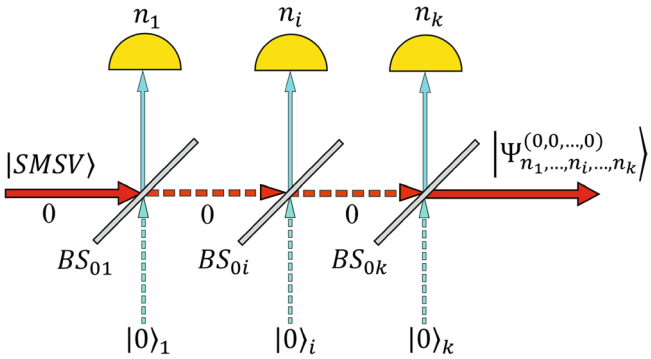

Figure 1. Optical scheme used to shape even/odd SCS of large amplitude with fidelity over 0.99. It consists of a sequence of k beam splitters with transmittance coefficient $t_i (i = 1, 2, \ldots, k)$ following one after another through which the original SMSV state with squeezing amplitude s passes forming the entangled hybrid state in Eq. (24). Part of the reflected photons $(n_1, n_2, \ldots, n_k)$ is simultaneously measured in auxiliary modes resulting in either even CV (Eq. (25)) in the case of $n_1 + n_2 + \cdots + n_k = 2m_N$ or odd CV (Eq. (26)) heralded states provided that $n_1 + n_2 + \cdots + n_k = 2m_N + 1$. The conditional CV states can approximate either an even or an odd SCSs under certain values of one parameter y_k defined by s and $t_i (i = 1, 2, \ldots, k)$.

PNR detector capable of resolving the number of photons to within one redirected by the BS from the initial SMSV state.

Subtraction of total either even $N_k = n_1 + n_2 + \cdots + n_k = 2m_N$ or odd $N_k = n_1 + n_2 + \cdots + n_k = 2m_N + 1$ number of photons from original SMSV state in an indistinguishable manner so all information about which Fock state of the original superposition the photons are subtracted is lost generates the whole family of heralded CV states of definite parity in Eqs. (25, 26). The projection of the hybrid entangled state in Eq. (24) onto Fock states can be realized by the simultaneous registration of $n_1 \ldots, n_i, \ldots n_k$ photons in k measurement modes by modern TES detectors resolution of which has been improved[37]. The measurement-induced CV states have a well-defined parity. The superpositions in Eq. (25) involve only even number states, while the CV states in Eq. (26) consist exclusively of odd number states. Therefore, the family can be divided into two subfamilies by its parity, namely, even in Eq. (25) and odd Eq. (26), respectively. As the state in Eq. (25) becomes SMSV state in Eq. (1) in the case of $m_N = 0$, the SMSV state belongs to an even subfamily. The success probabilities to realize the $2m_N, 2m_N + 1$ CV states follow from definition of the amplitudes of the entangled state in Eq. (27) $P^{(0,0,\ldots,0)}_{n_1,n_2,\ldots,n_k} = \left|C^{(0,0,\ldots,0)}_{n_1,n_2,\ldots,n_k}\right|^2/\cosh s$ with the normalization condition $\sum_{n_1,\ldots,n_{i,\ldots},n_k=0}^{\infty} P^{(0,0,\ldots,0)}_{n_1,n_2,\ldots,n_k} = 1$.

The optical scheme in Fig. 1 can be used for quantum engineering of measurement-induced even/odd SCSs. Indeed, such a task makes sense since the heralded CV states of definite parity may have photon distributions similar to even/odd SCSs ones which are given by.

$$|SCS_+\rangle = 2N_+(\beta)exp\left(-\beta^2/2\right)\sum_{n=0}^{\infty}\frac{\beta^{2n}}{\sqrt{(2n)!}}|2n\rangle, \tag{2}$$

$$|SCS_-\rangle = 2N_-(\beta)exp\left(-\beta^2/2\right)\sum_{n=0}^{\infty}\frac{\beta^{2n+1}}{\sqrt{(2n+1)!}}|2n+1\rangle, \tag{3}$$

where $N_\pm = \left(2\left(1 \pm exp\left(-2\beta^2\right)\right)\right)^{-1/2}$ are the corresponding normalization factors and $\beta > 0$ is an amplitude of the SCSs. For example, the difference between the heralded and target states is in that the amplitude β to the power of $2m\left(\beta^{2m}\right)$ in Eq. (2) unlike the parameter y_k to the power of $m\left(y_k^m\right)$ in Eq. (25). Instead of the difference between β^{2m} and y_k^m, the CV states in Eq. (25) have an additional factor either $(2(n + m_N))!/(n + m_N)!$ associated with the number of extracted photons which can compensate for the difference between β^{2m} and y_k^m. To estimate how close the measurement induced $2m_N, 2m_N + 1$ CV states can be to the target even/odd SCSs, one uses parameter fidelity $F_{2m_N} = \left|\langle SCS_+|\Psi^{(0,0,\ldots,0)}_{2m_N}\rangle\right|^2$ and $F_{2m_N+1} = \left|\langle SCS_-|\Psi^{(0,0,\ldots,0)}_{2m_N+1}\rangle\right|^2$ for two pure states. Ideal fidelity $F_{2m_N,max} = F_{2m_N+1,max} = 1$ can indicate on identity of the two states $|\Psi^{(0,0,\ldots,0)}_{2m_N}\rangle = |SCS_+\rangle$ and $|\Psi^{(0,0,\ldots,0)}_{2m_N+1}\rangle = |SCS_-\rangle$. We are interested in finding such conditions that provide the highest possible value of the fidelity, which nevertheless is less than one. In what follows, we do not use the subscript *max* for the highest possible fidelity.

The dependences of the maximum possible fidelities F_{2m_N}, F_{2m_N+1} of the CV states in Eqs. (25, 26) on the SCS amplitude β are shown in Fig. 2. The number of subtracted photons varies from 0 to 90 for even (Fig. 2a,b) and from 1 to 91 (Fig. 2c,d) for odd CV states. In general, the more photons are subtracted from the initial SMSV, the higher the fidelity of the generated even/odd SCSs with greater amplitude β. So, in the case of extracting more than 80 photons from original SMSV, even/odd SCSs of amplitude of more than 5 can be generated with fidelity exceeding 0.99. The maximum possible fidelity F_{2m_N}, F_{2m_N+1} solely depends on one parameter either $y_{2m_N}(\beta)$ or $y_{2m_N+1}(\beta)$. The parameters $y_{2m_N}(\beta)$ and $y_{2m_N+1}(\beta)$ that provide the fidelity values in Fig. 2 are shown in Fig. 3 in dependency on the SCS amplitude β. The obtained values of $y_{2m_N}(\beta)$ and $y_{2m_N+1}(\beta)$ can be used to select the BS transmittances t_i and also the squeezing amplitude s of the initial SMSV state. Note that the reverse rule is observed for values of $y_{2m_N}(\beta)$ and $y_{2m_N+1}(\beta)$. The more photons are extracted from SMSV state, the smaller the value of the parameter $y_{2m_N}(\beta)$ and $y_{2m_N+1}(\beta)$ is required to generate the target even/odd SCSs. If the value of the parameter y_k becomes less of either $y_{2m_N}(\beta)\left(y_k < y_{2m_N}(\beta)\right)$ or $y_{2m_N+1}(\beta)\left(y_k < y_{2m_N+1}(\beta)\right)$, then the generation of the even/odd SCSs with the fidelity shown in Fig. 2 is impossible for given value of β. This imposes certain restrictions on the squeezing amplitude s of the original SMSV state and, as a consequence, on the value of the initial parameter y_0 taking into account the fact that the passage of the SMSV state through the BSs reduces the value of y_0. So, in the case of using a system of one BS and PNR detector, initial value $y_0^{(1)}$ (here the superscript indicates a hub with the corresponding number of elements) of SMSV must meet the condition $y_0^{(1)} \geq y_{2m_N,2m_N+1}(\beta)$ to provide required fidelity in Fig. 2 for a preselected range of β. If a system with k BSs and PNR detectors is used in Fig. 1, then the following stronger constraint on $y_0^{(k)}$, i.e. $y_0^{(k)} \geq y_{2m_N,2m_N+1}(\beta)$, must be imposed to guarantee the fidelity shown in Fig. 2 for required values of β. The inequality can imply use of the SMSV state with larger squeezing amplitude s to provide the more value of $y_0^{(k)}$ on compared with $y_0^{(1)}$, i.e. $y_0^{(k)} > y_0^{(1)}$. It is also interesting to note a rather strong density of curves $y_{2m_N}(\beta)$ and $y_{2m_N+1}(\beta)$ at certain values of the SCS amplitude β in Fig. 3, especially, in the range of $0.11 \geq y_{2m_N,2m_N+1}(\beta) > 0$. This may mean that at a certain value of either $y_k = y_{2m_N}(\beta)$ or $y_k = y_{2m_N+1}(\beta)$, most of the measurement outcomes, except for measuring outcomes with a small number of photons including vacuum, can generate SCSs of certain amplitude with slightly different fidelities which can reduce the requirements for the PNR detector to resolve the number of photons. The idea of generating even/odd SCSs of large amplitude for almost any measurement outcome n greater than a certain value n_0, i.e. $n > n_0$ is promising and deserves separate consideration.

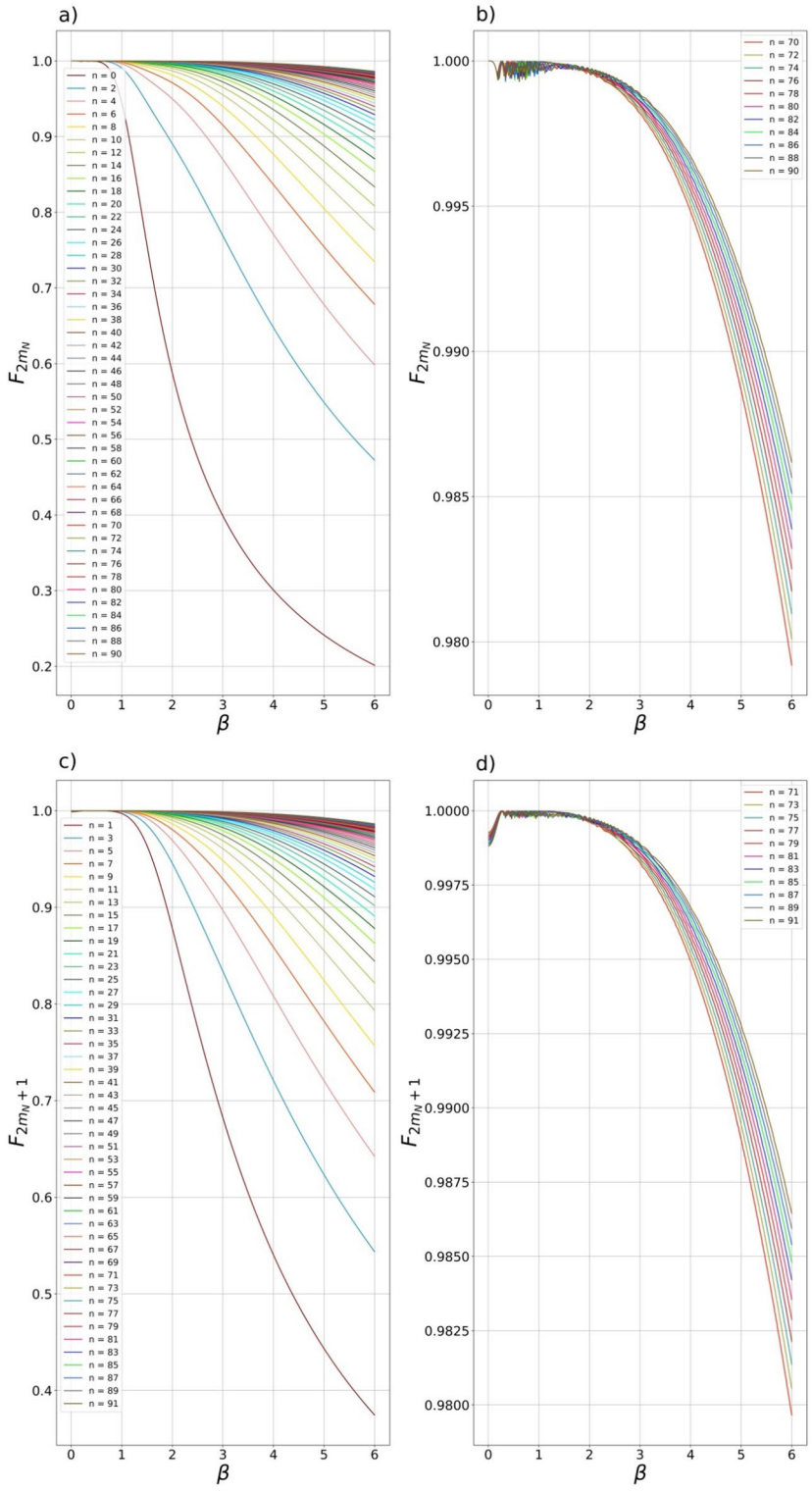

Figure 2. (**a**–**d**) Dependence of the even (**a**, **b**) F_{2m} and odd (**c**, **d**) F_{2m+1} fidelities between $2m, 2m+1-$ heralded CV states of definite parity and even/odd SCSs on the SCS amplitude β. The more photons n is measured in auxiliary modes, the higher fidelities F_n of the generated states is observed. Dependences of the fidelities of higher-order CV states with n from 70 up to 91 depending on β are separately shown in subfigures (**b**) и (**d**). The dependences on subfigures (**b**) и (**d**) allow for one to observe generation of even/odd SCSs with an amplitude greater than 5 with fidelity exceeding 0.99.

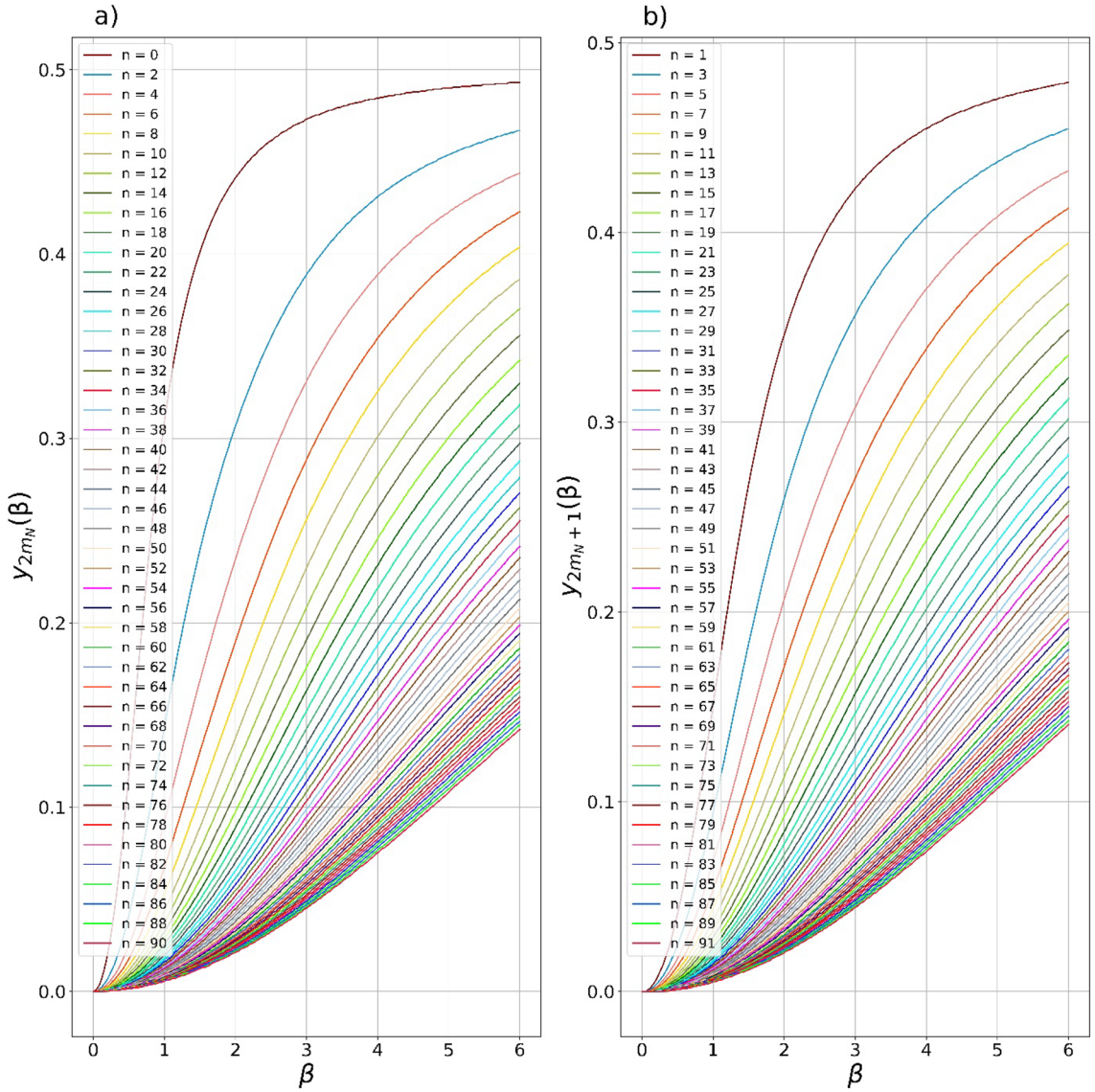

Figure 3. (**a**, **b**) $2m, 2m+1-$heralded states in Eqs. (25, 26) depend solely on one CV parameter $0 \leq y_k \leq 0.5$. The plots demonstrate the dependencies of the parameter (**a**) $y_{2m_N}(\beta)$ and (**b**) $y_{2m_N+1}(\beta)$ that provide the fidelities in Fig. 2 if either $y_k = y_{2m_N}(\beta)$ or $y_k = y_{2m_N+1}(\beta)$. The larger the number n of the extracted photons, the smaller the value of the parameters $y_{2m_N}(\beta)$ and $y_{2m_N+1}(\beta)$, moreover accompanied by an increase in the fidelity of the conditional states.

The success probabilities to conditionally generate $2m_1, 2m_1+1$ CV states in optical scheme with one BS and PNR detector follow from Eqs. (23) and are given by.

$$P^{(0)}_{2m_1} = \frac{1}{\text{coshs}}\left(\frac{1-t_1^2}{t_1^2}\right)^{2m_1} \frac{y_1^{2m_1}}{(2m_1)!} Z^{(2m_1)}(y_1), \tag{4}$$

$$P^{(0)}_{2m_1+1} = \frac{1}{\text{coshs}}\left(\frac{1-t_1^2}{t_1^2}\right)^{2m_1+1} \frac{y_1^{2m_1+1}}{(2m_1+1)!} Z^{(2m_1+1)}(y_1). \tag{5}$$

It is worth noting that the success probability of the measurement also depends on the BS parameter t_1, in contrast to the fidelity, which is completely determined by the value y_1. To evaluate the success probability to implement the even/odd SCSs one should take $y_1 = y_{2m_N}(\beta)$ in Eq. (4) and $y_1 = y_{2m_N+1}(\beta)$ in Eq. (5). The success probabilities both for arbitrary values of y_1 and for those providing SCSs generation fall rather quickly with increasing the parameter m_1, i.e. $P^{(0)}_{2m_1+2}/P^{(0)}_{2m_1} = \left((1-t_1^2)/t_1^2\right)^2 y_1^2((2m_1)!/(2m_1+2)!)\left(Z^{(2m_1+2)}(y_1)/Z^{(2m_1)}(y_1)\right)$

$\ll 1$, $\frac{P^{(0)}_{2m_1+3}/P^{(0)}_{2m_1+1} = \left(\left(1-t_1^2\right)/t_1^2\right)^2 y_1^2((2m_1+1)!/(2m_1+3)!)}{\left(Z^{(2m_1+3)}\left(y_1\right)/Z^{(2m_1+1)}\left(y_1\right)\right)} \ll 1$ involving the case of $y_1 = y_{2m_N}(\beta)$ and $y_1 = y_{2m_N+1}(\beta)$. The finding drastically reduces the generation rate of the even/odd SCSs of larger amplitude requiring more photon subtraction in setup with one BS and PNR detector.

Let us compare the success probabilities $P^{(0,0,\ldots,0)}_{n_1,n_2,\ldots,n_k}$ of the even/odd SCSs generation in configuration with k BSs and PNR detectors and ones $P^{(0)}_{n_1+n_2+\cdots+n_k}$ by equal subtraction of photons in both cases. Here, a superscript (0) indicates on the hub with one BS and PNR detector while a superscript $(0,0,\ldots,0)$ with k zeros is applied to show that k BSs and PNR detectors are used in the optical scheme in Fig. 1. The success probability to implement the CV states of definite parity in Eqs. (25, 26) becomes.

$$\begin{aligned} P^{(0,0,\ldots,0)}_{n_1,n_2,\ldots,n_k} &= \frac{1}{\cosh s}\prod_{l=1}^{k}\left(\frac{1-t_l^2}{t_l^2}\right)^{n_l}\frac{y_l^{n_l}}{n_l!}Z^{(n_1+n_2+\cdots+n_k)}\left(y_k\right) \\ &= P^{(0)}_{n_k/n_1,n_2,\ldots,n_{k-1}}P^{(0)}_{n_{k-1}/n_1,n_2,\ldots,n_{k-2}}\ldots P^{(0)}_{n_3/n_1,n_2}P^{(0)}_{n_2/n_1}P^{(0)}_{n_1}, \end{aligned} \tag{6}$$

where the conditional probability is given by.

$$P^{(0)}_{n_i/n_1,n_2,\ldots,n_{i-1}} = \left(\frac{1-t_i^2}{t_i^2}\right)^{n_i}\frac{y_i^{n_i}}{(n_i)!}\frac{Z^{(n_1+n_2+\cdots+n_i)}\left(y_i\right)}{Z^{(n_1+n_2+\cdots+n_{i-1})}\left(y_{i-1}\right)}, \tag{7}$$

obeying the normalization condition $\sum_{n_i=0}^{\infty}P^{(0)}_{n_i/n_1,n_2,\ldots,n_{i-1}} = 1$. Here, the quantity $P^{(0)}_{n_1}$ is presented in Eqs. (4, 5). The success probabilities for generating even/odd SCSs is obtained by taking either $y_k = y_{2m_N}(\beta)$ or $y_k = y_{2m_N+1}(\beta)$ heeding the relationship between y_i and $y_k (i < k)$ in Eq. (6) to get amounts $P^{(0,0,\ldots,0)}_{n_1,n_2,\ldots,n_k}\left(y_{2m_N}(\beta)\right)$ and $P^{(0,0,\ldots,0)}_{n_1,n_2,\ldots,n_k}\left(y_{2m_N+1}(\beta)\right)$, respectively. Substituting either $y_{2m_N}(\beta)$ or $y_{2m_N+1}(\beta)$ instead of y_k, one estimates the ratio of the success probabilities for the hub with one element $P^{(0)}_{n_1+n_2+\cdots+n_k}\left(y_{2m_N,2m_N+1}(\beta)\right)$ and k elements $P^{(0,0,\ldots,0)}_{n_1,n_2,\ldots,n_k}\left(y_{2m_N,2m_N+1}(\beta)\right)$ configured to generate even/odd SCSs.

$$\frac{P^{(0,0,\ldots,0)}_{n_1,n_2,\ldots,n_k}\left(y_{2m_N,2m_N+1}(\beta)\right)}{P^{(0)}_{n_1+n_2+\cdots+n_k}\left(y_{2m_N,2m_N+1}(\beta)\right)} = \left(t^{-2}\right)^{(k-1)n_1+(k-2)n_2+\ldots+n_{k-1}}\frac{(n_1+n_2+n_3\cdots+n_k)!}{(n_1)!(n_2)!\ldots(n_k)!}, \tag{8}$$

with the same number of extracted photons in both cases, where the hub with k elements composes of identical BSs $t_1 = t_2 \cdots = t_k = t$. When evaluating ratio in Eq. (8), we supposed that $y_0^{(1)} = y_0^{(k)}$ which is acceptable to compare two values. As can be seen from the relation, the following estimate $P^{(0,0,\ldots,0)}_{n_1,n_2,\ldots,n_k}\left(y_{2m_N,2m_N+1}(\beta)\right) \gg P^{(0)}_{n_1+n_2+\cdots+n_k}\left(y_{2m_N,2m_N+1}(\beta)\right)$ takes place, since there are two factors postulating the inequality. The factor $(n_1+n_2+n_3\cdots+n_k)!/(n_1)!(n_2)!\ldots(n_k)!$ makes a significant increasing contribution to the ratio of the probabilities in addition to the increasing multiplier $\left(t^{-2}\right)^{(k-1)n_1+(k-2)n_2+\ldots+n_{k-1}}$. But it is worth heeding the decrease in the transmittance coefficient t is limited by the corresponding condition on amount $y_0^{(k)}$ noted above. Substantial reducing the transmittance coefficient t can lead to impossibility of generating even/odd SCSs of certain amplitude with required high fidelity. Note also the inequality under study can be only increased in the case of $t_1 > t_2 > \ldots t_k$.

Let us consider in more detail the success probability to implement SCSs in a scheme with two identical BSs ($t_1 = t_2 = t$) and two PNR detectors. Then, for example, the success probability to generate even SCS can be written as.

$$P^{(0,0)}_{2m_1,2m_2} = \sqrt{1-4\left(\frac{y_{2m_N}(\beta)}{t^4}\right)^2}\left(\frac{1-t^2}{t^2}\right)^{2m_1+2m_2}\frac{1}{\left(t^2\right)^{2m_1}}\frac{\left(y_{2m_N}(\beta)\right)^{2m_1+2m_2}}{(2m_1)!(2m_2)!}Z^{(2m_1+2m_2)}\left(y_{2m_N}(\beta)\right), \tag{9}$$

in the case of total even number of detected photons $2m_1+2m_2 = 2m_N$ provided that both detectors have registered even Fock states $2m_1$ and $2m_2$, respectively. Here, the multiplier $1/\cosh s$ is expressed in terms of the parameter $y_{2m_N}(\beta) = t^4 y_0$. In Fig. 4(a,b), we show the dependence of the success probabilities to generate even SCSs for various even measurement outcomes registered by two PNR detectors provided that the total number of registered photons is 20, i.e. $2m_1+2m_2 = 20$. Here, the SCS amplitude range is selected from 2.2 to 3, where the appropriate large fidelity (Fig. 2a) is provided. Note that a further increase of the SCS amplitude $\beta > 3$ may lead to the impossibility of generating the corresponding SCS with the fidelity shown in Fig. 2a for the selected values of the BSs parameters $t_1 = t_2 = t$ since the value y_2/t^4 may exceed the threshold value 0.5. Numerical results confirm significant gain in the success probability when using two PNR detectors compared to one. All probabilities $P^{(0,0)}_{n_1,n_2}$ in Fig. 4a,b with $n_1 \neq 0$ exceed the probability to implement even SCS with one PNR detector. The dependence of $P^{(0,0)}_{0,2m_N}\left(y_{2m_N}(\beta)\right) \cong P^{(0)}_{2m_N}\left(y_{2m_N}(\beta)\right)$ (the difference between the probabilities is very insignificant and is related to the different values of input $y_0^{(2)} > y_0^{(1)}$ that should be applied that entails only slight increase of $P^{(0)}_{2m_N}\left(y_{2m_N}(\beta)\right)$ over $P^{(0,0)}_{0,2m_N}\left(y_{2m_N}(\beta)\right)$, i.e. $P^{(0)}_{2m_N}\left(y_{2m_N}(\beta)\right) > P^{(0,0)}_{0,2m_N}\left(y_{2m_N}(\beta)\right)$) is shown in Fig. 4a,b and takes on the lowest possible values of all the plots presented. As can be seen from the plots, the probability

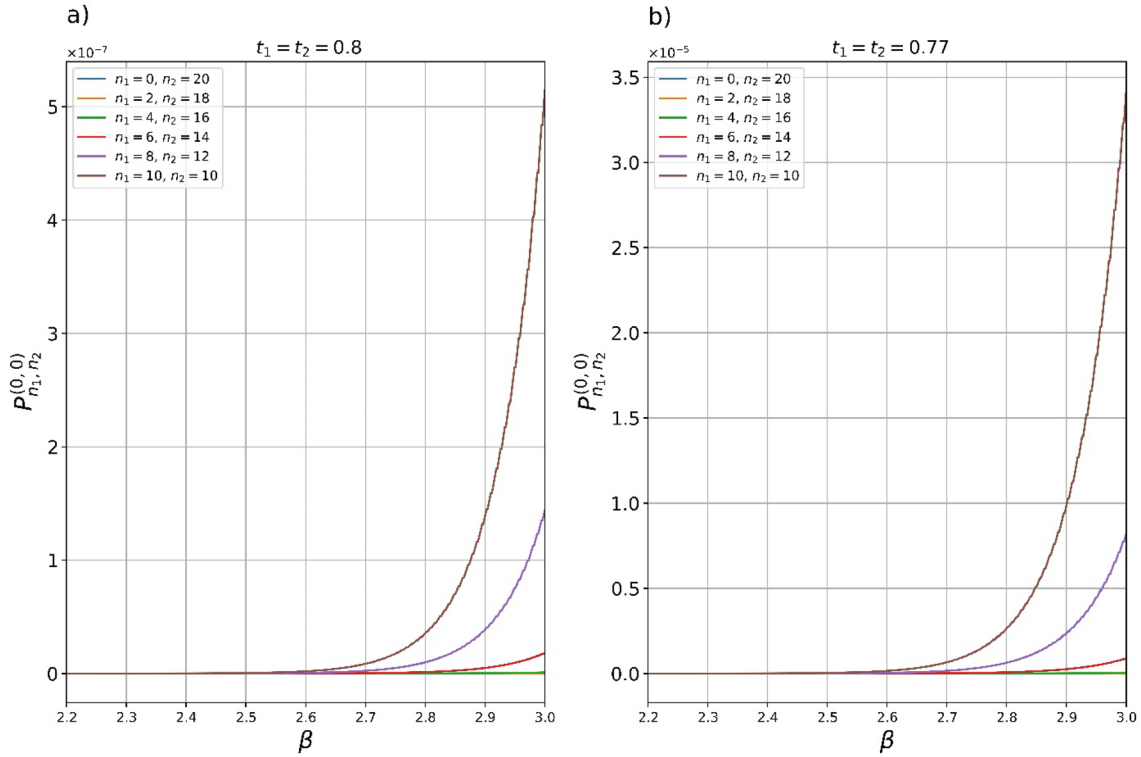

Figure 4. (**a**, **b**) Plots of the success probabilities $P^{(0,0)}_{n_1,n_2}\left(y_{20}(\beta)\right)$ (Eq. (6)) to generate even SCSs with the fidelity presented in Fig. 2a on output of the hub with two BSs and PNR detectors in the dependency on the SCS amplitude β. The plots are constructed for different BSs transmittance coefficients: (**a**) $t_1 = t_2 = 0.8$ and b) $t_1 = t_2 = 0.77$. Detection of only even photon states $n_1 = 2m_1$ and $n_2 = 2m_2$ is considered. The maximum possible probability $P^{(0,0)}_{10,10}\left(y_{20}(\beta)\right)$ is observed when $n_1 = 10$ and $n_2 = 10$. Moreover, the probability is several orders of magnitude higher than the probability $P^{(0,0)}_{0,20}\left(y_{20}(\beta)\right)$, which almost coincides with the probability $P^{(0)}_{20}\left(y_{20}(\beta)\right)$ of generating SCS in a scheme with one BS and PNR detector $\left(P^{(0,0)}_{0,20}\left(y_{20}(\beta)\right) \cong P^{(0)}_{20}\left(y_{20}(\beta)\right)\right)$. Transmission of more photons into the measurement modes (**b**) makes it possible to increase the success probability by almost two orders of magnitude.

$P^{(0,0)}_{10,10}$ significantly exceeds all other probabilities $P^{(0,0)}_{n_1,n_2}$ with $n_1 \neq n_2$ for definite values of β. The use of the BSs with a little lower transmittance coefficient (Fig. 4b) makes it possible to increase the success probability $P^{(0,0)}_{10,10}$ by almost two orders compared $P^{(0,0)}_{10,10}$ in Fig. 4a. Note also that the fidelity of the output state solely depends on the total number of extracted photons either $2m_N$ or $2m_N + 1$, in contrast to the success probability, which is also determined by the number of photons extracted by each PNR detector.

Thus, use of the multiple hub can provide, at least, two advantages over optical scheme with a single BS and PNR detection. PNR detectors are characterized by several different parameters, such as efficiency, maximum number of the detectable photons, photon number resolution, etc. Registration of a large number of photons by a single PNR detector can impose too high requirements on maximum number of detectable photons detected with single-photon resolution which can be quite difficult to implement in practice. The multiphoton state splitting realized by multi-element hub through a split of the measured light into several output measurement modes each of which measures a smaller number of photons avoids higher requirements for the PNR detection. So, the multiphoton state demultiplexing with two PNR detectors registering up to 10 photons with single-photon resolution each is more feasible compared to one PNR detector, which should resolve up to 20 photons with the same resolution. An even more advantageous situation can take place in the case of exact detection maximum, say, up to 50 photons by one PNR detector. Instead of measuring 50 photons by one PNR detector, one can make use of, for example, a hub with 5 BSs and PNR detectors capable of resolving up to 10 photons with single-photons resolution each. In addition to reducing the sensitivity requirements for the PNR detectors in a scheme with a large number of elements, multi-element hub provides a significant gain in the success probability. The gain can only exponentially increase with an increment in the number of elements in the hub.

The discussion presented above referred to the ideal operation of the measuring technique. Therefore, the obtained numerical results in the Figs. 2, 3, 4 can be classified as perfect, that is, those that can be observed under ideal experimental conditions without taking into account the imperfection of the experimental measurement technique. Taking into account the imperfection of measuring equipment can worsen the values of perfect parameters (SCS amplitude β, fidelity). Nevertheless, consideration of the optical scheme in Fig. 1 under ideal

conditions makes sense, since it allows one to find the perfect values of the parameters that one should strive for in the practical implementation of quantum engineering of even/odd SCSs.

Influence of the quantum efficiency of the PNR detector on perfect values of the SCS generator. In real experiments, PNR detectors can have rather high quantum efficiency, but not an ideal one, i.e. $\eta < 1$ that can lead to a deterioration of the characteristics of the output states. To estimate the level of the fidelity degradation of generated SCSs, one introduces even/odd positive-operator values measure (POVM) elements of the PNR detector.

$$\Pi_{2m} = \sum_{x=0}^{\infty} \begin{pmatrix} C_{2(m+x)}^{2m} \eta^{2m} (1-\eta)^{2x} |2(m+x)\rangle\langle 2(m+x)| + \\ C_{2(m+x)+1}^{2m} \eta^{2m} (1-\eta)^{2x+1} |2(m+x)+1\rangle\langle 2(m+x)+1| \end{pmatrix}, \tag{10}$$

$$\Pi_{2m+1} = \sum_{x=0}^{\infty} \begin{pmatrix} C_{2(m+x)+1}^{2m+1} \eta^{2m+1} (1-\eta)^{2x} |2(m+x)+1\rangle\langle 2(m+x)+1| + \\ C_{2(m+x+1)}^{2m+1} \eta^{2m+1} (1-\eta)^{2x+1} |2(m+x+1)\rangle\langle 2(m+x+1)| \end{pmatrix}, \tag{11}$$

where C_i^j is a binomial coefficient. Now, the fidelities $Fid_{2m}^{(0)}(\eta) = tr\left(\rho_{2m}^{(0)}(|SCS_+\rangle\langle SCS_+|)\right)$ and $Fid_{2m+1}^{(0)}(\eta) = tr\left(\rho_{2m+1}^{(0)}(|SCS_-\rangle\langle SCS_-|)\right)$, where tr means the trace operation, $\rho_{2m}^{(0)} = tr_2\left(\rho^{(0)}\Pi_{2m}(\eta)\right)$, $\rho_{2m+1}^{(0)} = tr_2\left(\rho^{(0)}\Pi_{2m+1}(\eta)\right)$ are the conditional states and $\rho^{(0)} = (BS_{12}(|SMSV\rangle_1|0\rangle_2))(BS_{12}(|SMSV\rangle_1|0\rangle_2))^+$ is an original one, where upper symbol $+$ in operator is responsible for the Hermitian conjugation operation, should be analyzed by their decomposing in terms of the powers of small parameter $1-\eta$ up to $(1-\eta)^2$, provided that quantum efficiency of modern PNR detectors is high enough $\eta \approx 1$ but $\eta < 1$

$$Fid_{2m}^{(0)}(\eta) = Fid_{2m}^{(0)}(\eta=1)\left(1 - (1-\eta)\frac{1-t_1^2}{t_1^2}\langle n\rangle_{2m} + (1-\eta)^2 f_{2,2m}^{(0)}\right), \tag{12}$$

$$Fid_{2m+1}^{(0)}(\eta) = Fid_{2m+1}^{(0)}(\eta=1)\left(1 - (1-\eta)\frac{1-t_1^2}{t_1^2}\langle n\rangle_{2m+1} + (1-\eta)^2 f_{2,2m+1}^{(0)}\right), \tag{13}$$

where the mean number of photons of the even/odd SCSs.

$$\langle n\rangle_{2m} = y\frac{Z^{(2m+1)}}{Z^{(2m)}}, \tag{14}$$

$$\langle n\rangle_{2m+1} = y\frac{Z^{(2m+2)}}{Z^{(2m+1)}}, \tag{15}$$

is calculated with $y = y_{2m_N}(\beta)$ for even SCSs and $y = y_{2m_N+1}(\beta)$ for odd SCSs. Second order terms in decompositions in Eqs. (12, 13) are defined as.

$$f_{2,2m}^{(0)} = \frac{\langle n\rangle_{2m}}{2}\left(\frac{1-t_1^2}{t_1^2}\right)^2\left(2\langle n\rangle_{2m} - \langle n\rangle_{2m+1}\left(1 - R_{2m}^{(0)}\right)\right), \tag{16}$$

$$f_{2,2m+1}^{(0)} = \frac{\langle n\rangle_{2m+1}}{2}\left(\frac{1-t_1^2}{t_1^2}\right)^2\left(2\langle n\rangle_{2m+1} - \langle n\rangle_{2m+2}\left(1 - R_{2m+1}^{(0)}\right)\right), \tag{17}$$

where $R_{2m}^{(0)} = \left|\langle SCS_+|\Psi_{2m+2}^{(0)}\left(y_{2m}\right)\rangle\right|^2 / \left|\langle SCS_+|\Psi_{2m}^{(0)}\left(y_{2m}(\beta)\right)\rangle\right|^2$ and $R_{2m+1}^{(0)} = \left|\langle SCS_-|\Psi_{2m+3}^{(0)}\left(y_{2m+1}(\beta)\right)\rangle\right|^2 / \left|\langle SCS_-|\Psi_{2m+1}^{(0)}\left(y_{2m+1}(\beta)\right)\rangle\right|^2$. Here, the fidelities $Fid_{2m}^{(0)}(\eta=1)$ and $Fid_{2m+1}^{(0)}(\eta=1)$ are those that are shown in Fig. 2. The success probabilities in detecting $2m, 2m+1$ photons and thereby generating even/odd SCSs in the output mode are given by

$$\begin{aligned} P_{2m}^{(0)}(\eta) &= \frac{\eta^{2m}}{\cosh s}\left(\frac{1-t_1^2}{t_1^2}\right)^{2m}\frac{y_1^{2m}}{(2m)!}\begin{pmatrix} \sum_{x_1=0}^{\infty}\left(\frac{1-t_1^2}{t_1^2}\right)^{2x_1}\frac{y_1^{2x_1}}{(2x_1)!}Z^{(2(m+x_1))}(y_1)(1-\eta)^{2x_1} + \\ \sum_{x_1=0}^{\infty}\left(\frac{1-t_1^2}{t_1^2}\right)^{2x_1}\frac{y_1^{2x_1}}{(2x_1)!}Z^{(2(m+x_1))}(y_1)(1-\eta)^{2x_1} \end{pmatrix} \\ &\approx \eta^{2m}P_{2m}^{(0)}(\eta=1)\left(1 + (1-\eta)\frac{1-t_1^2}{t_1^2}\langle n\rangle_{2m}\right), \end{aligned} \tag{18}$$

$$\begin{aligned} &BS_{0k}BS_{0k-1}\ldots BS_{0i}\ldots BS_{01}(|SMSV\rangle_0|0\rangle_1|0\rangle_2\ldots|0\rangle_i\ldots|0\rangle_k) \\ &= \frac{1}{\sqrt{\cosh s}}\sum_{n_1=0}^{\infty}\cdots\sum_{n_1=0}^{\infty}\cdots\sum_{n_k=0}^{\infty}(-1)^{n_1+n_2+\cdots+n_k}C_{n_1,n_2,\ldots,n_k}^{(0,0,\ldots,0)}|\Psi_{n_1,\ldots,n_i,\ldots,n_k}^{(0,0,\ldots,0)}\rangle_0|n_1\rangle_1\ldots|n_i\rangle_i\ldots|n_k\rangle_k, \end{aligned} \tag{19}$$

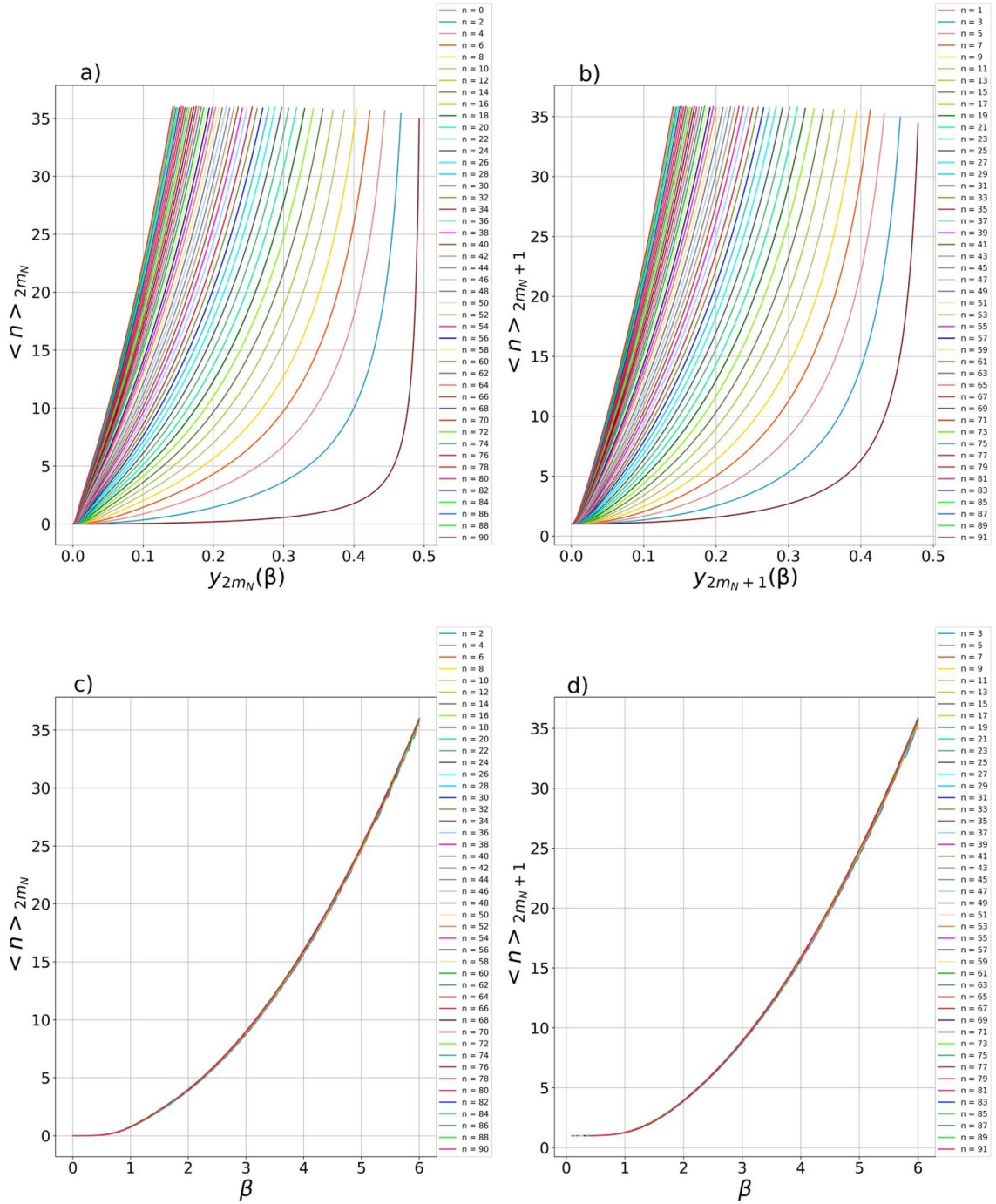

Figure 5. (**a**–**d**) Dependence of average number of photons (**a**) $\langle n \rangle_{2m_N}$ and (**b**) $\langle n \rangle_{2m_N+1}$ in generated CV states on parameters $y_{2m_N}(\beta)$ and $y_{2m_N+1}(\beta)$, respectively, which provide the maximum fidelity of the states with even/odd SCSs. When constructing (**c**) $\langle n \rangle_{2m_N}$ and (**d**) $\langle n \rangle_{2m_N+1}$ depending on the corresponding SCS amplitude β, the curves coincide with each other which confirms the rule for the SCSs i.e. $\langle n \rangle_{2m_N} \approx \beta^2$ and $\langle n \rangle_{2m_N+1} \approx \beta^2$.

where $P^{(0)}_{2m}(\eta = 1)$ and $P^{(0)}_{2m+1}(\eta = 1)$ are given by Eqs. (4, 5). As can be seen from the presented formulas, the fidelity is a deviation by a certain amount from the perfect value $\left(F^{(0)}_{2m,2m+1}(\eta = 1) > F^{(0)}_{2m,2m+1}(\eta)\right)$ in the case of small values of the quantum inefficiency $1 - \eta \ll 1$. The success probability is increased by the same amount compared to the perfect value $P^{(0)}_{2m,2m+1}(\eta) > P^{(0)}_{2m,2m+1}(\eta = 1)$.

The largest decreasing contribution to the fidelities in Eqs. (12, 13) proportional to $1 - \eta$ includes the product of the BS parameter $\left(1 - t_1^2\right)/t_1^2$ by the mean number of photons either $\langle n \rangle_{2m}$ or $\langle n \rangle_{2m+1}$. The mean number of photons in SCSs is known to be proportional to its amplitude squared i.e. $\langle n \rangle_{SCS} \sim \beta^2$ and the more the SCS

amplitude is, the greater the average number of photons is in it. To check the fact for the CV states of certain parity, the dependences of the mean number of photons in the generated states are shown in the Fig. 5. The plots in Fig. 5a,b are the dependence of the mean number of photons on the parameter $y_{2m_N}(\beta), y_{2m_N+1}(\beta)$ which provides the fidelities in Fig. 2, while the graphs in Fig. 5c,d also show the mean number of photons in the CV states of definite parity but in dependence on the SCS amplitude β. The form of the curves in Fig. 5a,b is related to the fact that their arguments are defined in different ranges of change y (see Fig. 3a, b). So, the arguments $y_{90}(\beta)$ and $y_{91}(\beta)$ for the states $|\Psi_{90}^{(0,0,\ldots,0)}\rangle$ and $|\Psi_{91}^{(0,0,\ldots,0)}\rangle$, respectively, change in a smallest range (Fig. 3a,b), which entails that the plots of $\langle n\rangle_{90}$ and $\langle n\rangle_{91}$ are maximally shifted to the left. As can be seen the Fig. 5c,d the condition $\langle n\rangle_{2m} \approx \beta^2, \langle n\rangle_{2m+1} \approx \beta^2$ is met (the curves on the graphs almost coincide regardless of the number of extracted photons), which also indicates the that the generated CV states of a certain parity can approximate even/odd SCSs with high fidelity (Fig. 2). The maximum number of average number of photons is limited to a value of just over 35 for the maximum considered number of subtracted photons, namely 90 and 91. Note that the graphs in Fig. 5 are applicable to a hub regardless of the number of its elements, that is, both to the hub with one and k elements.

The contribution of the mean number of photons can be partly compensated for by the BS parameter provided that a beam splitter different from the balanced one that is, with $t_1 > 1/\sqrt{2}$ is used to guarantee the performance of the condition $\left(1-t_1^2\right)/t_1^2 < 1$. Then, the factor reducing the fidelity can be reduced to zero in the case of use of the HTBS with $t_1 \to 1$, when the BS parameter $\left(1-t_1^2\right)/t_1^2$ tends to zero, thereby nullifying contribution of the mean number of photons to the overall fidelity in Eqs. (12, 13) that can provide perfect values of the fidelity, i.e.$Fid_{2m}^{(0)}(\eta) \approx Fid_{2m}^{(0)}(\eta=1)$ and $Fid_{2m+1}^{(0)}(\eta) \approx Fid_{2m+1}^{(0)}(\eta=1)$. Unfortunately, the strategy of using HTBS has a significant drawback. It follows from the formulas (18, 19) that the success probability just depends on the same BS multiplier $\left(1-t_1^2\right)/t_1^2$ in the appropriate degree either $2m$ or $2m+1$ as well as its perfect values in Eqs. (4, 5). The power dependence can very quickly reduce the perfect values of the success rate and to zero which confirms the inapplicability of the HTBS strategy to extracting a large number of photons from the initial SMSV state. Indeed, the HTBS redirects a single photon into measurement mode with probability $\sim \left(1-t_1^2\right)$, while n photons can be redirected with probability $\sim \left(1-t_1^2\right)^n \approx 0$ in the case of $t_1 \to 1$. In general, the relationship between the fidelity of the output CV state and its success probability can be reflected by the following expressions: $\Delta F_{2m}^{(0)}(\eta)\cdot\Delta P_{2m}^{(0)}(\eta) \approx (1-\eta)^2\left(\left(1-t_1^2\right)/t_1^2\right)^2\langle n\rangle_{2m}F_{2m}^{(0)}(\eta=1)\cdot P_{2m}^{(0)}(\eta=1)$ and $\Delta F_{2m+1}^{(0)}(\eta)\cdot\Delta P_{2m+1}^{(0)}(\eta) \approx (1-\eta)^2\left(\left(1-t_1^2\right)/t_1^2\right)^2\langle n\rangle_{2m+1}F_{2m+1}^{(0)}(\eta=1)\cdot P_{2m+1}^{(0)}(\eta=1)$, where $\Delta F_{2m,2m+1}^{(0)}(\eta) = F_{2m,2m+1}^{(0)}(\eta=1) - F_{2m,2m+1}^{(0)}(\eta)$ and $\Delta P_{2m,2m+1}^{(0)}(\eta) = P_{2m,2m+1}^{(0)}(\eta) - P_{2m,2m+1}^{(0)}(\eta=1)$ are the differences between the perfect and those values that are realized in the case of using an inefficient PNR detector.

The result can be extended to the case of an optical hub consisting of k elements, which leads to rather cumbersome expressions for the fidelity and the success probability. Nevertheless, for qualitative conclusions, it is sufficient to consider the case of k detectors with the same quantum efficiency η and limit our consideration to the first order in quantum inefficiency $1-\eta$, which gives.

$$Fid_{2m_N,2m_N+1}^{(0,0,\ldots,0)}(\eta) = Fid_{2m_N,2m_N+1}^{(0,0,\ldots,0)}(\eta=1)\left(1-(1-\eta)\frac{1-t_1^2t_2^2\ldots t_k^2}{t_1^2t_2^2\ldots t_k^2}\langle n\rangle_{2m_N,2m_N+1}\right), \tag{20}$$

$$P_{2m_N,2m_N+1}^{(0,0,\ldots,0)}(\eta) = P_{2m_N,2m_N+1}^{(0,0,\ldots,0)}(\eta=1)\left(1+(1-\eta)\frac{1-t_1^2t_2^2\ldots t_k^2}{t_1^2t_2^2\ldots t_k^2}\langle n\rangle_{2m_N,2m_N+1}\right), \tag{21}$$

where $Fid_{2m_N,2m_N+1}^{(0,0,\ldots,0)}(\eta=1)$ and $P_{2m_N,2m_N+1}^{(0,0,\ldots,0)}(\eta=1)$ are the perfect values of the fidelity and the success probability. It follows from the expressions that the values of the fidelity and success probability act in discord with respect to each other, that is, the fidelity decreases and the success probability increases by the same amount. The value is proportional both to the mean number of photons in the generated state, which follow from the curves in Fig. 5, and to the hub's parameter $\left(1-t_1^2t_2^2\ldots t_k^2\right)/t_1^2t_2^2\ldots t_k^2$. In general, the multiplier $\left(1-t_1^2t_2^2\ldots t_k^2\right)/t_1^2t_2^2\ldots t_k^2$ is more than the factor $\left(1-t_1^2\right)/t_1^2$ present in Eqs. (12, 13), i.e. $\left(1-t_1^2t_2^2\ldots t_k^2\right)/t_1^2t_2^2\ldots t_k^2 \geq \left(1-t_1^2\right)/t_1^2$ which reduces the possibilities for the hub parameter to decrease the contribution of the mean number of photons. So, in the case of using the same BSs so that the condition $t_1 = t_2 = \cdots = t_k = t$ takes place, the hub's parameter becomes lowering $\left(\left(1-t^{2k}\right)/t^{2k} < 1\right)$ in the case of $t > 1/\sqrt[2k]{2}$. As in the case of a one-element hub, it is possible to achieve perfect values for the fidelity $Fid_{2m_N,2m_N+1}^{(0,0,\ldots,0)}(\eta) \approx Fid_{2m_N,2m_N+1}^{(0,0,\ldots,0)}(\eta=1)$ in the case of $\left(1-t_1^2t_2^2\ldots t_k^2\right)/t_1^2t_2^2\ldots t_k^2 \to 1$ which is guaranteed to lead to a strategy of using k HTBSs with $t_1 \to 1, t_2 \to 1, \ldots, t_k \to 1$. The strategy with HTBSs is hardly practical for the quantum state engineering of the even/odd SCSs, since the perfect values of the success probability tend to zero in the case of subtracting a large number of photons (say, more of 20) even though (as shown above) the strategy with multiphoton state demultiplexing gives a certain gain to the final success probability (Eq. (21)) due to the multiplier $(1-\eta)\left(\left(1-t_1^2t_2^2\ldots t_k^2\right)/t_1^2t_2^2\ldots t_k^2\right)\langle n\rangle_{2m_N,2m_N+1}$. However, the strategy with HTBSs (or partial use of HTBSs) may become practical when extracting a small number of photons (say, less than 10). It is also possible to estimate deviations of the parameter values from their perfect values taking into account $Fid_{2m,2m+1}^{(0)}(\eta=1) > Fid_{2m,2m+1}^{(0)}(\eta)$ and $P_{2m,2m+1}^{(0)}(\eta) > P_{2m,2m+1}^{(0)}(\eta=1)$, namely, $\Delta F_{2m_N}^{(0,0,\ldots,0)}(\eta)\cdot\Delta P_{2m_N}^{(0,0,,0)}(\eta) \approx (1-\eta)^2\left(\left(1-t_1^2t_2^2\ldots t_k^2\right)/t_1^2t_2^2\ldots t_k^2\right)^2\langle n\rangle_{2m_N}F_{2m_N}^{(0,0,\ldots,0)}(\eta=1)\cdot P_{2m_N}^{(0,0,\ldots,0)}(\eta=1)$ and $\Delta F_{2m_N+1}^{(0,0,,0)}(\eta)\cdot\Delta P_{2m_N+1}^{(0,0,\ldots,0)}(\eta) \approx$

$(1-\eta)^2\left(\left(1-t_1^2t_2^2\ldots t_k^2\right)/t_1^2t_2^2\ldots t_k^2\right)^2\langle n\rangle_{2m_N+1}F^{(0,0,\ldots,0)}_{2m_N+1}(\eta=1)\cdot P^{(0,0,\ldots,0)}_{2m_N+1}(\eta=1)$, where the quantities $\Delta F^{(0,0,\ldots,0)}_{2m_N,2m_N+1}(\eta)$ and $\Delta P^{(0,0,\ldots,0)}_{2m_N,2m_N+1}(\eta)$ are the differences between the perfect and those values that are obtained in the practical case of using an inefficient PNR detector $\Delta F^{(0,0,\ldots,0)}_{2m_N,2m_N+1}(\eta)=F^{(0,0,\ldots,0)}_{2m_N,2m_N+1}(\eta=1)-F^{(0,0,\ldots,0)}_{2m_N,2m_N+1}(\eta)$ and $\Delta P^{(0,0,\ldots,0)}_{2m_N,2m_N+1}(\eta)=P^{(0,0,\ldots,0)}_{2m_N,2m_N+1}(\eta=1)-P^{(0,0,\ldots,0)}_{2m_N,2m_N+1}(\eta=1)$, respectively.

The dependences in Fig. 5 allow us to estimate the contribution of the decreasing term to the fidelity of the output states generated with inefficient PNR detectors. Let us take the maximum observed value $\langle n\rangle_{90}=\langle n\rangle_{91}\approx 35$ for estimation. Then, the decreasing factor can be evaluated by $\approx 35\left(\left(1-t_1^2\right)/t_1^2\right)$ in a scheme with one BS and PNR detector (Eqs. (12, 13)) and $\approx 35\left(\left(1-t_1^2t_2^2\right)/t_1^2t_2^2\right)$ (Eq. (20)) in setup with two BSs and PNR detectors in the case subtraction of either 90 for generation of even SCS or 91 photons for generation of odd SCS. The reducing factor $35\left(\left(1-t_1^2\right)/t_1^2\right)$ can take the following values: 8.21 for $t_1=0.9$; 3.78 for $t_1=0.95$ and 1.44 for $t_1=0.98$. In the case of a hub with two identical BSs ($t_1=t_2=t$) and PNR detectors, the decreasing multiplier $35\left(\left(1-t_1^2t_2^2\right)/t_1^2t_2^2\right)$ can take on the following values: 18.35 for $t=0.9$; 7.97 for $t=0.95$ and 2.94 for $t=0.98$. If we take value of the quantum efficiency $\eta=0.98$ [33], then one have the following fidelities: $Fid^{(0)}_{90,91}(\eta)\approx 0.8358\cdot Fid^{(0)}_{90,91}(\eta=1)$ for $t_1=0.9$; $Fid^{(0)}_{90,91}(\eta)\approx 0.9244\cdot Fid^{(0)}_{90,91}(\eta=1)$ for $t_1=0.95$; $Fid^{(0)}_{90,91}(\eta)\approx 0.9712\cdot Fid^{(0)}_{90,91}(\eta=1)$ for $t_1=0.98$. One can choose the value of the SCS amplitude β in such a way that $Fid^{(0)}_{90,91}(\eta=1)>0.99$ (Fig. 2), but it does not corroborate the utility of the strategy, since the success probability is proportional to either $\left(1-t_1^2\right)^{90}$ or $\left(1-t_1^2\right)^{91}$ and can take on very small values, much less of $<10^{-20}$. Comparing the values of decreasing multipliers, it can be noted that they can only increase with an increase in the number of the hub's elements. So, one can evaluate from Eq. (20) $Fid^{(0,0)}_{90}(\eta)\approx 0.8406\cdot Fid^{(0,0)}_{45,45}(\eta=1)$ for $t_1=t_2=0.95$ and $\eta=0.98$.

In order to take advantage of two-element hubs in terms of substantial gain in the success probability keeping the fidelity of the output SCS at an acceptable level, it is worth reducing the number of photons subtracted. As follows from Fig. 4, an increase in the success probability is provided when two PNR detectors detect the same or almost the same number of photons. So, in the case of generating even SCS of amplitude of $\beta=3$ by detecting 20 photons with two PNR detectors, we approximately have $\langle n\rangle_{20}\approx 8$ and $Fid^{(0,0)}_{20}(\eta=0.98)\approx 0.9162\cdot Fid^{(0,0)}_{10,10}(\eta=1)$ for $t_1=t_2=0.9$. The success probability of the event takes the values $\sim 10^{-9}$. If one reduces the number of extracted photons by half (say 10 photons) with help of two BSs with $t_1=t_2=0.95$, then one can estimate the final reduction factor as 0.9727 and the output fidelity becomes $Fid^{(0,0)}_{10}(\eta=0.98)\approx 0.9727\cdot Fid^{(0,0)}_{5,5}(\eta=1)$. The success probability of the event is estimated at the level of $\sim 10^{-7}$ which can be evaluated as more practical in the quantum engineering of even/odd SCSs of amplitudes $\beta=2.5$. Progress in the development of the qualitative PNR detectors with quantum efficiency $\eta>0.98$ can improve the above estimates. Note that the term acceptable is used in comparison with the success probability of spontaneous parametric down conversion whose effectiveness is usually bounded above by a value 10^{-6}. In a real experimental case, the efficiency of the conversion can be even lower, on the order of 10^{-8}. In addition to the quantum inefficiency inherent to PNR detectors, losses in detector couplers can also worsen the above estimates due to the loss of part of the photons. So, if we take into account the coupling efficiency of each detector, then the total quantum efficiency of the PNR detector should be reduced by an appropriate amount, for example, to $\eta=0.9$, which reduces the above estimates when extracting 10 and 20 photons with two PNR detectors. Estimates for generating even/odd SCSs of amplitudes in the range from 2.5 to 3 by subtraction from 10 to 20 photons from the initial SMSV state can also be extended to the case of photon resolution by three PNR detectors. The use of three PNR detectors for the measurement-induced generation of the SCSs is more effective for brighter input SMSV state (with squeezing more than $10dB$). So in case of $t_1=t_2=t_3=0.9$ the estimates following from the formula (6) (it follows from Eq. (21) the contribution of the quantum efficiency of the PNR detector to the success probability is minimal) give the success probability in the range $P^{(0,0,0)}_{6,6,6}(\eta=0.98)\approx 10^{-4}$ for SCS amplitude $\beta=2.5$ to $P^{(0,0,0)}_{4,4,4}(\eta=0.98)\approx 10^{-3}$ for $\beta=2.5$. Note that, as follows from the Eq. (20), the fidelity of the output CV state can only decrease in the case compared to the one in the case of using two PNR detectors.

Discussion

Study of quantum effects in physical systems of macroscopic sizes is largely driven by introduction of Schrödinger cat states[1] as one of the most fundamental issue of quantum mechanics. It is no occasional that solution of the problem spurred serious interest to multiphoton states that could contain, on average, larger number of photons not limiting to a few to observe nonclassical features on the macroscopic states. Here, we have demonstrated the possibility of generating a whole family of multiphoton states of a certain parity generated from related to them SMSV state by extraction of multiphoton state from original state and registering them in the measurement modes of a multi-element hub. Redirecting photons in an indistinguishable manner, followed by probabilistic detection of a certain number of photons, redistributes the input distribution of the SMSV state to a new associated with the original. New CV states of definite parity with a larger mean number of photons in Eqs. (25, 26) have potential applications in quantum state engineering and optical quantum metrology. The generated states of the CV family of definite parity are characterized by only one parameter $0<y<0.5$, which exclusively depends on the squeezing amplitude of the original SMSV. In the scheme with one BS and PNR detector, the input parameter y_0 is multiplied by the BS transmittance coefficient squared, thereby lowering it by the corresponding value. In the scheme with multiphoton state demultiplexing, the reduction of y_0 can be more destructive due to successive multiplication by BS transmittance coefficients squared. We have shown that for each multiphoton state $|m_N\rangle$

subtracted from original SMSV there is a parameter value $y_{2m_N}(\beta)$ for even and $y_{2m_N+1}(\beta)$ for odd number of subtracted photons which provides the maximum fidelity of the CV state of a certain parity with even/odd SCS of amplitude β. In order to achieve the perfect fidelity of the SCSs generator, it is necessary to ensure the fulfillment of the condition $y_k = y_{2m_N,2m_N+1}(\beta)$. Thus, the squeezing amplitude s and BS's parameters t_i can be chosen appropriately to ensure the condition $y_k = y_{2m_N,2m_N+1}(\beta)$. From a practical point of view, the important point is that the values of $y_{2m_N,2m_N+1}(\beta)$ decrease with an increase of the number of the detected photons.

Control over the success probability is possible since it largely depends on the number of photons extracted by each detector, in contrast to the fidelity of the output state, which is solely determined by the total number of photons detected. Therefore, use of the multiphoton state demultiplexing by means of use of multi-element hub makes sense to greatly increase the success probability without affecting the fidelity of the output state. The use of only one BS and detector leads to a rather small values of the success probability $\left(10^{-20} >\right)$ of even/odd SCSs generation of large amplitude, when a sufficiently large number (> 50) of photons is subtracted. Greater redirection of photons of original SMSV state into measurement modes due to increased reflectance coefficients of the BSs is additional factor raising the success probability of the required event. But the strategy with BSs with increased reflectance coefficients should be accompanied by an increase in the squeezing amplitude of the initial SMSV and has a restrictive effect due to the inability to achieve the required condition $y_k = y_{2m_N,2m_N+1}(\beta)$ if a large number of BSs is used. In addition, use of several PNR detectors instead of one reduces the requirements imposed on the maximum number of detected photons registered with single-photon resolution. In general, strategy with multiple hub is more effective and promising for the quantum engineering of high-fidelity ≥ 0.99 even/odd SCSs of amplitude ≥ 5 with perfect PNR detectors. In general, the number of the subtracted photons can be increased (say up to 10^6) which leads to an increase in the amplitude of the generated even/odd SCSs with high fidelity > 0.99.

Consideration of an optical scheme in Fig. 1 with ideal PNR detection allows for one to find maximum possible values of the output parameters of the CV states and the conditions under which they could be observed. These perfect values can no longer be improved by any means in optical scheme in Fig. 1, they can only be worsened in their practical implementation due to the imperfection of measuring technology. In the case of practical quantum engineering of even/odd SCSs with inefficient PNR detectors, fidelity and success probability can become competing parameters which is analytically expressed. Use of the highly transmitting BSs generates the even/odd SCSs with fidelity close to perfect but only at the expense of a sharp decrease of the success probability since the multiphoton state has less chance of appearing in the measurement modes. An increase in the success probability is possible by redirecting more photons into the measurement modes but it reduces the fidelity of the even/odd SCSs. A trade-off between the values of the output characteristics (fidelity and success probability) can be achieved by subtraction of smaller photonic state (say, up to 20 photons) from original SMSV state in scheme with two BSs and PNR detectors to generate even/odd SCSs of less amplitudes ≤ 3. Practical quantum engineering of even/odd large-amplitude ≥ 5 high-fidelity ≥ 0.99 SCSs by subtraction of large (say, 100 photons) with help of multiple hub currently is a challenge. Note the recent work[37], where researchers were able to accurately resolve $0 - 100$ photons by three TESs, each capable of detecting maximum of 37 photons. By post-selecting data, they achieved error rates below 1% on photon number measurements beyond 30 photons per measurement channel not perturbing the measurement distribution. Progress in practical quantum engineering of large-amplitude and high-fidelity SCSs may stem from the measurement technology developed in the work.

Methods

Passing SMSV state through the optical hub. To trace the influence of the optical hub on the unitary evolution of the initial SMSV state in Fig. 1, it is worth using the system of transformations on the creation operators imposed by each of BS_i: $a_0^+ \to t_i a_0^+ - r_i a_i^+$, $a_i^+ \to r_i a_0^+ + t_i a_i^+$, where a_0^+ is the creation operator of the light field propagating in 0 mode and a_i^+ is the creation operator of i light field generated by BS_i. The transformations are the basis to derive output entangled state. Let us first apply them to situatio with one BS and one PNR detector, i.e. $BS_{01}(|SMSV\rangle_0|0\rangle_1)$. Using the linearity of the beam splitter quantum operator, expanding the action of superposition of the creation operators $\left(t_1 a_0^+ - r_1 a_1^+\right)^l |00\rangle_{01}$ and collecting all the terms for the Fock state in the first mode $|n\rangle_1$, one obtains the following hybrid entangled state.

$$BS_{01}(|SMSV\rangle_0|0\rangle_1) = \frac{1}{\sqrt{\cosh s}} \sum\nolimits_{n=0}^{\infty} C_n^{(0)} |\Psi_n^{(0)}\rangle_0 |n\rangle_1, \tag{22}$$

with amplitudes.

$$C_n^{(0)} = (-1)^n \left(\frac{1-t_1^2}{t_1^2}\right)^{\frac{n}{2}} \frac{y_1{}^{\frac{n}{2}}}{\sqrt{n!}} \begin{cases} \sqrt{Z^{(2m)}\left(y_1\right)}, ifn = 2m \\ \sqrt{Z^{(2m+1)}\left(y_1\right)}, ifn = 2m+1 \end{cases}, \tag{23}$$

while the CV states of definite parity present in the hybrid entangled state in Eq. (22) follow directly from those below. Also details of the mathematical function $Z\left(y_1\right)$, its derivatives of order $2m$, $2m+1$ and its argument y_1 are presented below. Generalization to the case of the passage of the SMSV state through a series of BSs arranged one behind the other as shown in Fig. 1 can be carried out according to a similar algorithm when the output entangled state from the current BS is the input for the next. Finally, output entangled state produced by series of k BSs over SMSV inputted into mode 0 is given by

$$BS_{0k}BS_{0k-1}\ldots BS_{0i}\ldots BS_{01}(|SMSV\rangle_0|0\rangle_1|0\rangle_2\ldots|0\rangle_i\ldots|0\rangle_k)$$
$$=\frac{1}{\sqrt{\cosh s}}\sum_{n_1=0}^{\infty}\ldots\sum_{n_i=0}^{\infty}\ldots\sum_{n_k=0}^{\infty}(-1)^{n_1+n_2+\cdots+n_k}C^{(0,0,\ldots,0)}_{n_1,n_2,\ldots,n_k}|\Psi^{(0,0,\ldots,0)}_{n_1,\ldots,n_i,\ldots,n_k}\rangle_0|n_1\rangle_1\ldots|n_i\rangle_i\ldots|n_k\rangle_k, \tag{24}$$

where BS_{0i} means the beam splitter operator mixing modes 0 and i. Here, the CV states with even total number $N_k=n_1+n_2+\cdots+n_k=2m_N$ of photons reflected to ancillary measurement modes are presented by.

$$|\Psi^{(0,0,\ldots,0)}_{n_1,\ldots,n_i,\ldots,n_k}\rangle=|\Psi^{(0,0,\ldots,0)}_{2m_N}\rangle=\frac{1}{\sqrt{Z^{(2m_N)}(y_k)}}\sum_{n=0}^{\infty}\frac{y_k^n}{\sqrt{(2n)!}}\frac{(2(n+m_N))!}{(n+m_N)!}|2n\rangle \tag{25}$$

while the CV states with odd total number $N_k=n_1+n_2+\cdots+n_k=2m_N+1$ of photons redirected to ancillary measuring modes are given by.

$$|\Psi^{(0,0,\ldots,0)}_{n_1,\ldots,n_i,\ldots,n_k}\rangle=|\Psi^{(0,0,\ldots,0)}_{2m_N+1}\rangle=\sqrt{\frac{y_k}{Z^{(2m_N+1)}(y_k)}}\sum_{n=0}^{\infty}\frac{y_k^n}{\sqrt{(2n+1)!}}\frac{(2(n+m_N+1))!}{(n+m_N+1)!}|2n+1\rangle. \tag{26}$$

Amplitudes of the entangled state in Eq. (24) are given by.

$$C^{(0,0,\ldots,0)}_{n_1,n_2,\ldots,n_k}=\prod_{l=1}^{k}\left(\frac{1-t_l^2}{t_l^2}\right)^{\frac{n_l}{2}}\frac{y_l^{\frac{n_l}{2}}}{\sqrt{n_l!}}\begin{cases}\sqrt{Z^{(2m_N)}(y_k)}, if N_k=2m_N\\ \sqrt{Z^{(2m_N+1)}(y_k)}, if N_k=2m_N+1\end{cases} \tag{27}$$

Here, the following function $Z(y)=1/\sqrt{1-4y^2}$ and its derivative $Z^{(m)}=d^mZ/dy^m$ with respect to the parameter $y=t^2\tanh s/2$ determined through the experimental parameters (t,s) are introduced. If only one beam splitter is used in Fig. 1, then the argument of the $Z(y)$ becomes $y_1=t_1^2\tanh s/2$, that is, $Z(y_1)=1/\sqrt{1-4y_1^2}$, it differs from the original y_0 by the value t_1^2 i.e. $y_1=t_1^2y_0$. By definition, the parameter y_1 can also take values in the range $0<y_1<0.5$ in the case of $s>0$. Note that the case $y_1=0$ is realized either in the absence of the SMSV state at the input to the BS ($s=0$) or in the case of reflection of all photons into the second auxiliary mode that is, when $t_1=0, r_1=1$, while the case of $y_1=0.5$ can only appears in the non-physical case of $s\to\infty$ and $t_1=1$. The passage of the original SMSV through $i-$ BS leads to a change of the input parameter y_0 to y_i as $y_0\to y_i=\left(t_1^2t_2^2\ldots t_i^2\right)\tanh s/2=t_1^2t_2^2\ldots t_i^2y_0=t_i^2y_{i-1}$ in Eqs. (25–27). The parameter y_{i-1} acquires an additional reducing factor t_i^2 after CV state has passed the next i BS i.e. $y_i=t_i^2y_{i-1}$. Finally, output state's parameter y_k used in Eqs. (25–27) becomes $y_k=\left(t_1^2t_2^2\ldots t_i^2\ldots t_k^2\right)\tanh s/2=t_1^2t_2^2\ldots t_i^2\ldots t_k^2y_0$ after the initial SMSV state goes through all k beam splitters. Thus, the action of the system of k successive BSs causes a decrease in the initial parameter y_0 in $t_1^2t_2^2\ldots t_i^2\ldots t_k^2$ times, i.e. $y_k/y_0=t_1^2t_2^2\ldots t_i^2\ldots t_k^2$ and function Z depends on y_k, i.e. $Z(y_k)=1/\sqrt{1-4y_k^2}$. The limiting values of the parameter y_k can be taken in the case of either $s=0$ or $t_i=0$ leading to $y_k=0$ or in the case of $s\to\infty, t_1=t_2=\cdots=t_i=\ldots t_k=1$ resulting in $y_i=0.5$ which are not of interest. Note that the CV states $|\Psi_n^{(0)}\rangle$ present in the hybrid entangled state in Eq. (22) follow directly from CV states in Eqs. (25, 26).

Data availability

The datasets used and/or analysed during the current study available from the corresponding author (S.A.P.) on reasonable request.

Received: 18 December 2022; Accepted: 17 February 2023
Published online: 09 March 2023

References

1. Schrödinger, E. Die gegenwärtige situation in der quantenmechanik. *Naturwissenschaften* **23**, 807–812 (1935).
2. Sanders, B. C. Entangled coherent states. *Phys. Rev. A* **45**, 6811–6815 (1992).
3. Gerry, C. C. & Knight, P. L. Quantum superpositions and Schrödinger cat states in quantum optics. *Am. J. Phys.* **65**, 964–974 (1997).
4. Wenger, J., Hafezi, M., Grosshans, F., Tualle-Brouri, R. & Grangier, P. Maximal violations of bell inequalities using continuous-variable measurement. *Phys. Rev. A* **67**, 012105 (2003).
5. Wineland, D. J. Nobel lecture: Superposition, entanglement, and raising Schrödinger's cat. *Rev. Mod. Phys.* **85**, 1103 (2013).
6. van Enk, S. J. & Hirota, O. Entangled coherent states: Teleportation and decoherence. *Phys. Rev. A* **64**, 022313 (2001).
7. Wang, X. Quantum teleportation of entangled coherent states. *Phys. Rev. A* **64**, 022302 (2001).
8. Cochrane, P. T., Milburn, G. J. & Munro, W. J. Macroscopically distinct quantum-superposition states as a bosonic code for amplitude damping. *Phys. Rev. A* **59**, 2631 (1999).
9. Ralph, T. C., Gilchrist, A., Milburn, G. J., Munro, W. J. & Glancy, S. Quantum computing with optical coherent states. *Phys. Rev. A* **68**, 042319 (2003).
10. Sangouard, N. *et al.* Quantum repeaters with entangled coherent states. *J. Opt. Soc. Am. B* **27**, A137–A145 (2010).
11. Podoshvedov, S. A. Efficient quantum teleportation of unknown qubit based on DV-CV interaction mechanism. *Entropy* **21**, 150 (2019).
12. Joo, J., Munro, W. J. & Spiller, T. P. Quantum metrology with entangled coherent states. *Phys. Rev. Lett.* **107**, 083601 (2011).
13. Podoshvedov, S. A. & An, N. B. Designs of interactions between discrete- and continuous- variable states for generation of hybrid entanglement. *Quantum Inf. Process.* **18**, 68 (2019).

14. Dakna, M., Anhut, T., Opatrny, T., Knöll, L. & Welsch, D. G. Generating Schrödinger-cat-like state by means of conditional measurement on a beam splitter. *Phys. Rev. A* **55**, 3184–3194 (1997).
15. Dakna, M., Knöll, D. & Welsch, D. G. Quantum state engineering using conditional measurement on a beam splitter. *Eur. Phys. J. D* **3**, 295–308 (1998).
16. Ourjoumtsev, A., Tualle-Brouri, R., Laurat, J. & Grangier, P. Generating optical Schrödinger kittens for quantum information processing. *Science* **312**, 83–86 (2006).
17. Podoshvedov, S. A. Elementary quantum gates in different bases. *Quantum Inf. Process.* **15**, 3967–3993 (2016).
18. Gerrits, T. *et al.* Generation of optical coherent-state superpositions by number-resolved photon subtraction from the squeezed vacuum. *Phys. Rev. A* **82**, 031802 (2010).
19. Takahashi, H. *et al.* Generation of large-amplitude coherent-state superposition via ancilla-assisted photon subtraction. *Phys. Rev. Lett.* **101**, 233605 (2008).
20. Podoshvedov, S. A. & Kim, J. Testing quantum mechanics against macroscopic realism using the output of $\chi 2$ nonlinearity. *Phys. Rev. A* **74**, 033810 (2006).
21. Ourjoumtsev, A., Ferreyrol, F., Tualle-Brouri, R. & Grangier, P. Preparation of non-local superpositions of quasi-classical light states. *Nat. Phys.* **5**, 189–192 (2009).
22. Huang, K. *et al.* Optical synthesis of large-amplitude squeezed coherent-state superpositions with minimal resource. *Phys. Rev. Lett.* **115**, 023602 (2015).
23. Gerry, C. C., Benmoussa, A. & Bruno, K. M. Single-mode squeezed vacuum states as approximate Schrödinger phase cats: Relation to su(1,1) phase operators. *J. Opt. B* **5**, 109–115 (2003).
24. Giancy, S. & de Vasconcelos, H. M. Methods for producing optical coherent state superpositions. *J. Opt. Soc. Am. B* **25**, 712–733 (2008).
25. Podoshvedov, S. A. & Kim, J. Dense coding by means of the displaced photon. *Phys. Rev. A* **77**, 032319 (2008).
26. Sychev, D. V. *et al.* Entanglement of optical Schrödinger cat states. *Nat. Photonics* **11**, 379–382 (2017).
27. Ulanov, A. E., Fedorov, I. A., Sychev, D., Grangier, P. & Lvovsky, A. I. Loss-tolerant state engineering for quantum-enhanced metrology via the reverse Hong-Ou-Mandel effect. *Nat. Commun.* **7**, 11925 (2015).
28. Israel, Y. *et al.* Entangled coherent states created by mixing squeezed vacuum and coherent light. *Optica* **6**, 753–757 (2019).
29. Takase, K., Yoshikawa, J., Asavanant, W., Endo, M. & Furusawa, A. Generation of optical Schrödinger's cat states by generalized photon subtraction. *Phys. Rev. A* **103**, 013710 (2021).
30. Mikheev, E. V., Pugin, A. S., Kuts, D. A., Podoshvedov, S. A. & An, N. B. Efficient production of large-size optical Schrödinger cat states. *Sci. Rep.* **9**, 14301 (2019).
31. Podoshvedov, S. A. & Podoshvedov, M. S. Entanglement synthesis based on the interference of a single-mode squeezed vacuum and a delocalized photon. *J. Opt. Soc. Am. B* **38**, 1341–1349 (2021).
32. Kuts, D. A. & Podoshvedov, S. A. Entangled states shaping with CV states of definite parity. *Sci. Rep.* **12**, 1558 (2022).
33. Lita, A. E., Miller, A. J. & Nam, S. W. Counting near-infrared single-photons with 95% efficiency. *Opt. Express* **16**, 3032–3040 (2008).
34. Fukuda, D. *et al.* Titanium-based transition-edge photon number resolving detector with 98% detection efficiency with index-matched small-gap fiber coupling. *Opt. Express* **19**, 870–875 (2011).
35. Sridhar, N. *et al.* Direct measurement of the Wigner function by photon-number-resolving detection. *J. Opt. Soc. Am. B* **31**, B34–B40 (2014).
36. Gerrits, T. *et al.* Extending single-photon optimized superconducting transition edge sensors beyond the single-photon counting regime. *Opt. Express* **20**, 23798–23810 (2012).
37. Eaton, M. *et al.* Resolution of 100 photons and quantum generation of unbiased random numbers. *Nat. Photon.* **17**, 106–111 (2023).

Acknowledgements

MSP, SAP and SPK are supported by the Ministry of Science and Higher Education of the Russian Federation on the basis of the FSAEIHE SUSU (NRU) (Agreement No. 075-15- 2022-1116).

Author contributions

S.A.P. contributed to the conception of the idea and development of mathematical apparatus. M.S.P. have performed all the numerical simulations and created all plots and took part in discussion of the results obtained. S.A.P. wrote the draft of the manuscript. S.P.K carried out general control of the work and reviewed the manuscript.

Competing interests

The authors declare no competing interests.

Additional information

Correspondence and requests for materials should be addressed to S.A.P.

Reprints and permissions information is available at www.nature.com/reprints.

Publisher's note Springer Nature remains neutral with regard to jurisdictional claims in published maps and institutional affiliations.